JOURNAL OF APPLIED ELECTROCHEMISTRY 19 (1989) 231–238

Dissolution of tin in the presence of Cl^- ions at pH 4

M. DROGOWSKA*, L. BROSSARD†, H. MÉNARD*

*Département de Chimie, 2500 boul. Université, Sherbrooke, Québec, Canada J1K 2R1

†Institut de recherche d'Hydro-Québec (IREQ), 1800 montée Ste-Julie, Varennes, Québec, Canada J0L 2P0

Received 18 May 1988; revised 15 August 1988

The anodic dissolution of tin, investigated in an acidic solution at pH 4 containing 0.1–1 M NaCl at 25° C, displays Tafel behavior as long as the electrode surface is bare ($E \leqslant -0.5$ V vs SCE). The main characteristics can be derived from the proposed dissolution mechanism, i.e. $(\partial E/\partial \log i)_{a_{Cl^-}} = 40$ mV/d.c., $(\partial \log i/\partial a_{Cl^-})_E \approx 1$ and $(\partial i/\partial \omega)_{E,a_{Cl^-}} \approx 0$. The mechanism involves two consecutive steps, each corresponding to the transfer of one electron, the second step being rate determining. For E values anodic to ≈ -0.5 V vs SCE partial coverage of the surface by a corrosion product is observed and the behavior is no longer Tafelian. From 0.4 to 1 V vs SCE, a plateau current is observed on log i vs E curves and the anode is completely covered by a corrosion product. Results obtained with a rotating disc electrode suggest that the rate-determining step of the dissolution process in this region of potential is the diffusion of an ionic species into the solution.

1. Introduction

Tin, an amphoteric metal, reacts to both acids and alkalines but is relatively resistant to neutral or near-neutral media. Used as an electrodeposited coating on steel, copper or nickel, it presents very large surface areas to corrosive environments. Potential–pH diagrams [1–3] show the degree of corrosion occurring in acid and alkaline solutions in contrast to the good stability in neutral solutions. In acidic conditions, the behavior of tin changes from passivity to corrosion at pH 5–4, which is in the acid rain range.

The high hydrogen overpotential of Sn implies that the pure metal will dissolve only slightly in acids free from air or other oxidizing agents and thus, corrosion can be controlled by the oxygen supply rate. However, in large amounts oxidants may practically stop corrosion and bring about passivation. Corrosion increases if tin is in contact with a metal with a low hydrogen overpotential and accelerates if small quantities of impurity elements, such as those in grades of commercial purity tin, are present [4, 5].

An anodic film formed on the tin surface can markedly influence the mode of corrosive attack [6–8] and the presence of different ions may modify the dissolution processes. Unlike most metals, tin is passivated in moderately strong halogen acid solutions [9–11]. This is probably due to the formation of basic salts of the type $SnOHCl \cdot H_2O$ whose stability is limited to a small range of potential, pH and halogen activity. The anodic behavior of tin in chloride solutions has been very little studied [11–15]. The corrosion of tin by many anions in neutral aqueous solutions was investigated by Hoar [11] who concluded that chloride is the most aggressive. Black spots are formed on tin by salt solutions; the latter give no precipitate with stannous ions.

More recently, the anodic dissolution of tin in acidic chloride solutions at pH $\leqslant$ 2.9 has been studied by Johnson and Liu using steady-state E–i data and valence measurements [12]. The apparent valence of the dissolving metal varied from about 0.4 to 2.4 and was a function of both the electrolyte and the current density. The authors proposed a reaction mechanism involving stepwise oxidation of Sn to $SnCl_2$ followed by a chemical reaction to form $SnCl_3^-$. The normal valence number of 2 for Sn ions was found [14, 13] with tin amalgam where neither anodic formation nor dispersion of tin particles in the electrolyte occur. The authors suggest that an apparent valence of less than 2 will be measured if some tin is lost and does not contribute to the faradic current.

Stirrup and Hampson [15] investigated the anodic behavior of tin in 0.1–5 M HCl solutions using the rotating disc technique. They found that the dissolution reaction had a Tafel value of 64 mV decade^{-1} and proposed a reaction mechanism of simultaneous two-electron transfer to form $SnCl^+$ species.

This work investigates the influence of chloride anions on anodic tin dissolution in aqueous solutions of pH4 at 25° C and containing 0.1–1 M NaCl. The rotating disc electrode is used while the nature of the changes occurring on the electrode surface during oxidation is clarified by semi-quantitative energy dispersive X-ray analysis and scanning electron microscopy.

2. Experimental details

The measurements were made in a conventional two-compartment, three-electrode electrochemical cell using a rotating disc electrode of 0.15 cm^2 surface, cut from a polycrystalline tin rod (Johnson Matthey Chem. Ltd, grade 1) and set in a Kel-F holder. The electrode surface was polished with an alumina suspension and rinsed in distilled water. The reference

0021-891X/89 $03.00 + .12

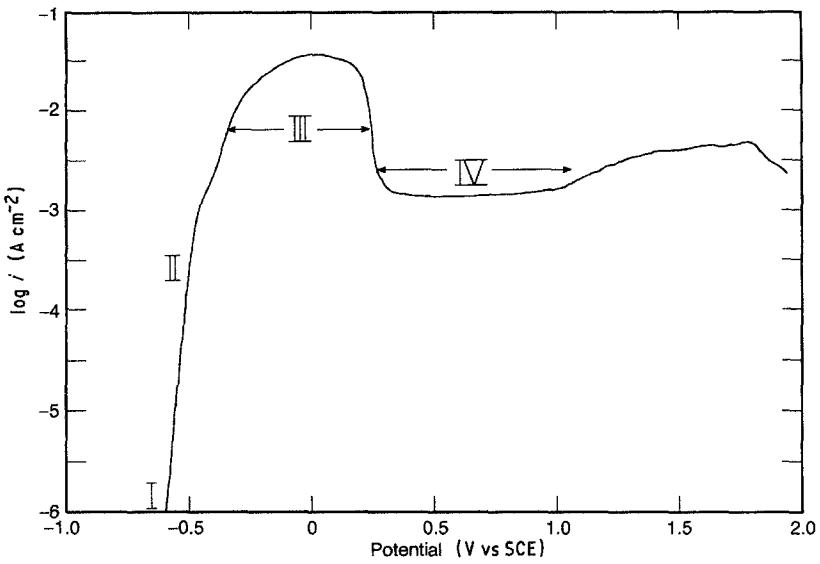

Fig. 1. Potentiodynamic curve of log i vs E in 0.5 M NaCl solution at pH 4 for a rotating disc electrode at 1000 rpm. The potential sweep rate is 5 mV s^{-1}. Region I: corrosion potential region; region II: Tafel region; region III: maximum current region; region IV: plateau current region.

electrode was a saturated calomel electrode separated from the main compartment by a bridge with a Luggin capillary tube; all potentials quoted in this paper are given with reference to this electrode. The auxiliary electrode was a platinum grid separated from the main compartment.

Solutions of 0.1–1 M NaCl (Baker analyzed reagent grade) were prepared and set at pH 4 using HCl. No buffer or support electrolyte was used. Before each measurement the solutions were deoxygenated with nitrogen, which was maintained above the solution at all times. All experiments were carried out at 25° C.

The potential applied to the working electrode by a PAR273 potentiostat was controlled by a pulse generator with a fast rise time and an accurate amplitude stability PAR175 universal programmer. The current–time transients were recorded under Commodor PCII microcomputer control using GPIB-PC-2A interface or, for microsecond records, under Computerscope interface (R.C. Electronics Inc.). Electrode rotation was performed using an Analytical Rotator Pine Instrument.

3. Results and discussion

Figure 1 shows a typical anodic potentiodynamic curve obtained with a rotating disc electrode of tin at 1000 rpm in 0.5 M NaCl solution at pH 4 and a sweep rate of 5 mV s^{-1}. The curve may be arbitrarily divided into four regions: (I) the electrode at its corrosion potential (E_{corr}), i.e. −0.606 V (open circuit potential); (II) linear relationship between log I and E with a Tafel slope of 40 mV $decade^{-1}$; (III) a broad oxidation peak observed having a maximum of 32 mA cm^{-2}; (IV) a plateau current (current density = 1.6 mA cm^{-2}) observed between +0.4 and +1.0 V. The present investigation focuses on regions I, II and IV.

3.1. *Corrosion potential region*

At the beginning of the measurements, the rotating disc electrode was immersed in the solution with the potentiostat already turned on at −0.8 V to remove any oxides from the surface. The electrode was then left on open circuit. The corrosion potential reached

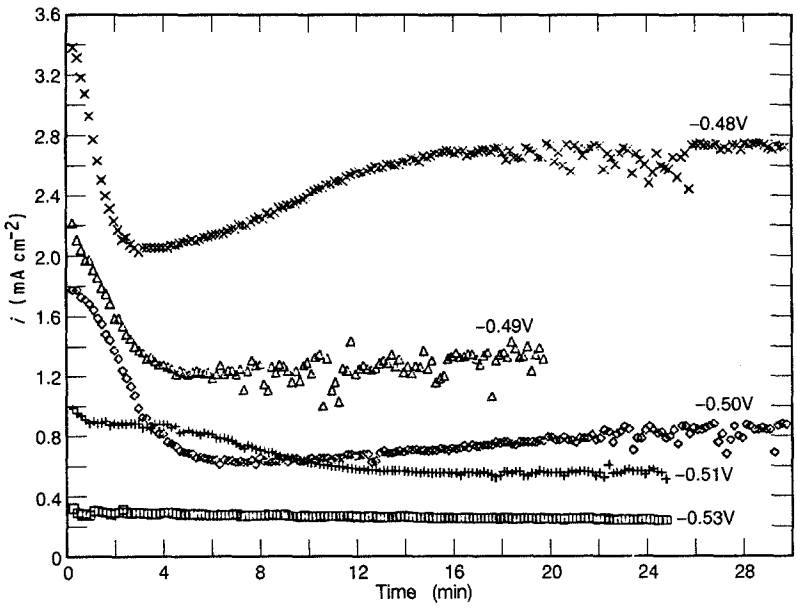

Fig. 2. Influence of the applied potential on the current vs time transients in 1 M NaCl solution. The potential step starts from E_{corr}. ω = 1000 rpm.

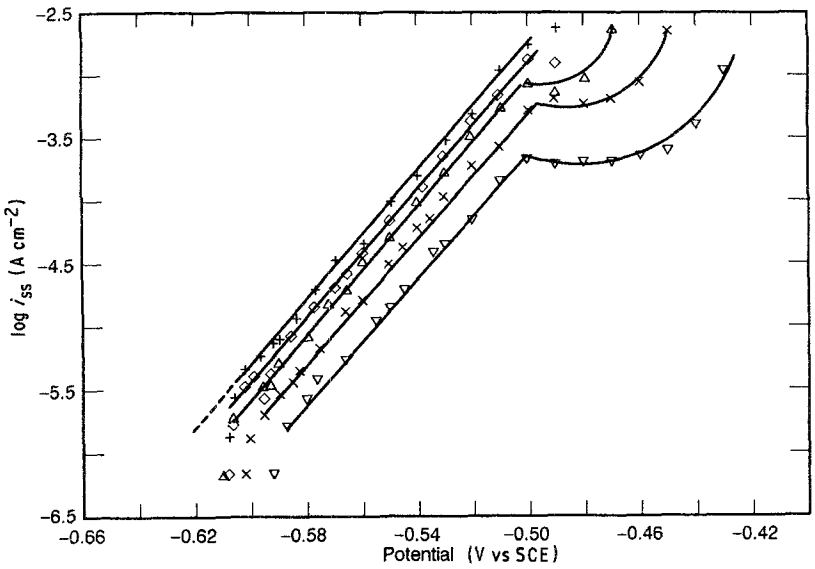

Fig. 3. Log i_{ss} vs E curves at different NaCl concentrations (M): + 1.0; ◇ 0.7; △ 0.5; × 0.3; ▽ 0.1. i_{ss} is the steady-state current density obtained under potentiostatic control. ω = 1000 rpm.

steady values in about 20 min and remained quite stable. During this period no changes on the electrode surface were observed. The corrosion potential values for 0.1–1 M NaCl solutions are given in Table 1. No change of E_{corr} occurred for the different selected electrode rotation speeds (ω) between 400 and 6000 rpm. The increase in concentration of the solution from 0.1 to 1 M NaCl shifted the corrosion potential towards a negative value, i.e. from −0.588 to −0.620 V, while the tin corrosion rate remained quite constant (Table 1), i.e. $i_{corr} \approx 1.7\,\mu A\,cm^{-2}$. The corrosion current, i_{corr}, was calculated from the extrapolation of the linear part of the log I vs E relationship (region II) to E_{corr} values.

The corrosion potentials are close to the equilibrium potential [1, 4] of the reactions

$$Sn + H_2O = SnO + 2H^+ + 2e^- \quad (1)$$
(solid, black)

$$E^0 = -0.104 - 0.0591pH$$
$$= -0.582\,V \text{ vs SCE, pH 4}$$

$$Sn + 2H_2O = SnO + 4H^+ + 4e^- \quad (2)$$
(solid, black)

$$E^0 = -0.106 - 0.0591pH$$
$$= -0.584\,V \text{ vs SCE, pH 4}$$

Generally, the initial net anodic process is a mixture of both reactions which have very close electrode potentials. The oxides formed must be in approximate equilibrium with stannous and stannic ions according to the oxide solubility, which increases with increasing $[H^+]$. The solubility of Sn(II) is greater than that of Sn(IV) [2]

$$SnO(s) + 2H^+ = Sn^{2+} + H_2O, \quad k = 11.8 \quad (3)$$

$$SnO_2(s) + 4H^+ = Sn^{4+} + 2H_2O,$$
$$k = 2.1 \times 10^{-8} \quad (4)$$

This difference may be increased by the presence of chloride ions

$$SnO(s) + 2H^+ + 4Cl^- = 2SnCl_4^{2-} + H_2O,$$
$$k = 5.8 \times 10^2 \quad (5)$$

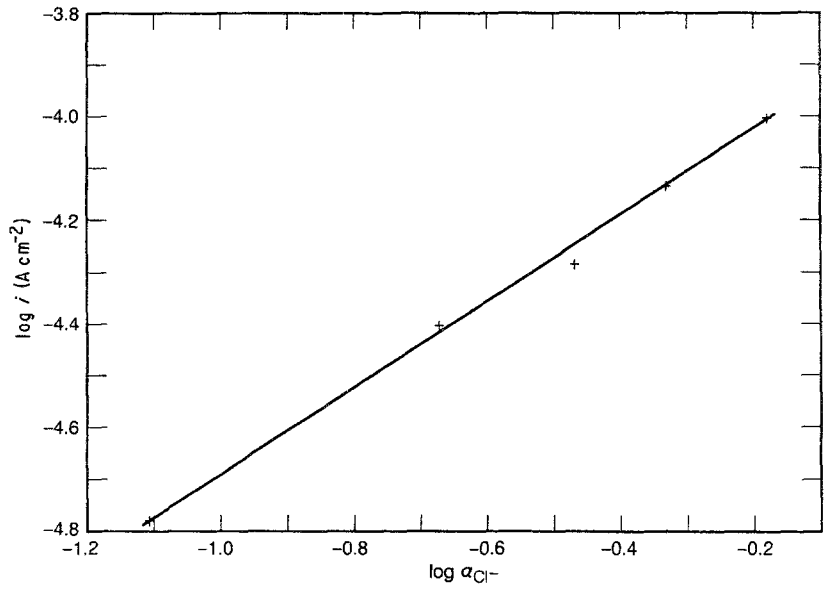

Fig. 4. Log i against log a_{Cl^-} at an applied potential of −0.55 V and ω = 1000 rpm. i and E values are obtained from the curves given in Fig. 3 for E = −0.55 V.

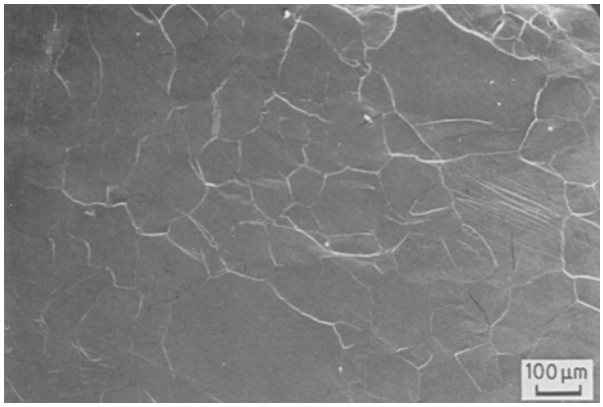

Fig. 5. Tin electrode surface prior to immersion. Magnification 52.5 ×.

$$SnO_2(s) + 4H^+ + 6Cl^- = SnCl_6^{2-} + 2H_2O, \quad k = 5.4 \times 10^{-8} \qquad (6)$$

At equilibrium, $SnOHCl \cdot H_2O$ is the only stable solid Sn(II) species, SnO being unstable with respect to SnO_2

$$SnOHCl \cdot H_2O(s) + H^+ + 3Cl^- = SnCl_4^{2-} + 2H_2O, \quad k = 5.8 \times 10^{-2} \qquad (7)$$

The double layer capacity of the tin electrode at E_{corr} increases from $14\,\mu F\,cm^{-2}$ at 0.1 M NaCl to $39\,\mu F\,cm^{-2}$ at 1 M NaCl (Table 1). This behavior is tentatively ascribed to the specific adsorption of Cl^- anions on the tin surface, which is consistent with the shift of E_{corr} in the negative direction at higher NaCl concentrations.

Table 1. Influence of chloride ion concentration on E_{corr}, i_{corr} and C_{dl}

NaCl chloride ion concentration (M)	*Corrosion potential (E_{corr}) (V)*	*Corrosion current (i_{corr}) ($\mu A\,cm^{-2}$)*	*Double layer capacity at E_{corr} (C_{dl}) ($\mu F\,cm^{-2}$)*
0.1	−0.588	1.7	14
0.3	−0.596	1.3	
0.5	−0.606	1.7	29
0.7	−0.611	1.8	
1	−0.620	1.7	39

3.2. *Tafel region*

To investigate the anodic dissolution of tin, current vs time curves were plotted at different values of constant applied potential in a concentration range from 0.1 to 1 M NaCl, the potential step starting from E_{corr}. Those presented in Fig. 2 were obtained for potentials ranging from −0.53 to −0.48 V at $\omega = 1000$ rpm in 1 M NaCl solution. In this range, the dissolution current and its variation with time are larger as the applied potential becomes more anodic. For example, at $E = -0.48$ V the current density drops from $\approx 3.5\,mA\,cm^{-2}$ at $t = 0$ to $\approx 2\,mA\,cm^{-2}$ at $t \approx 3$ min; for t larger than ≈ 3 min, the current density (i) increases with time to reach a plateau value at $t \approx 20$ min. At $E = -0.53$ V, the current density decreases

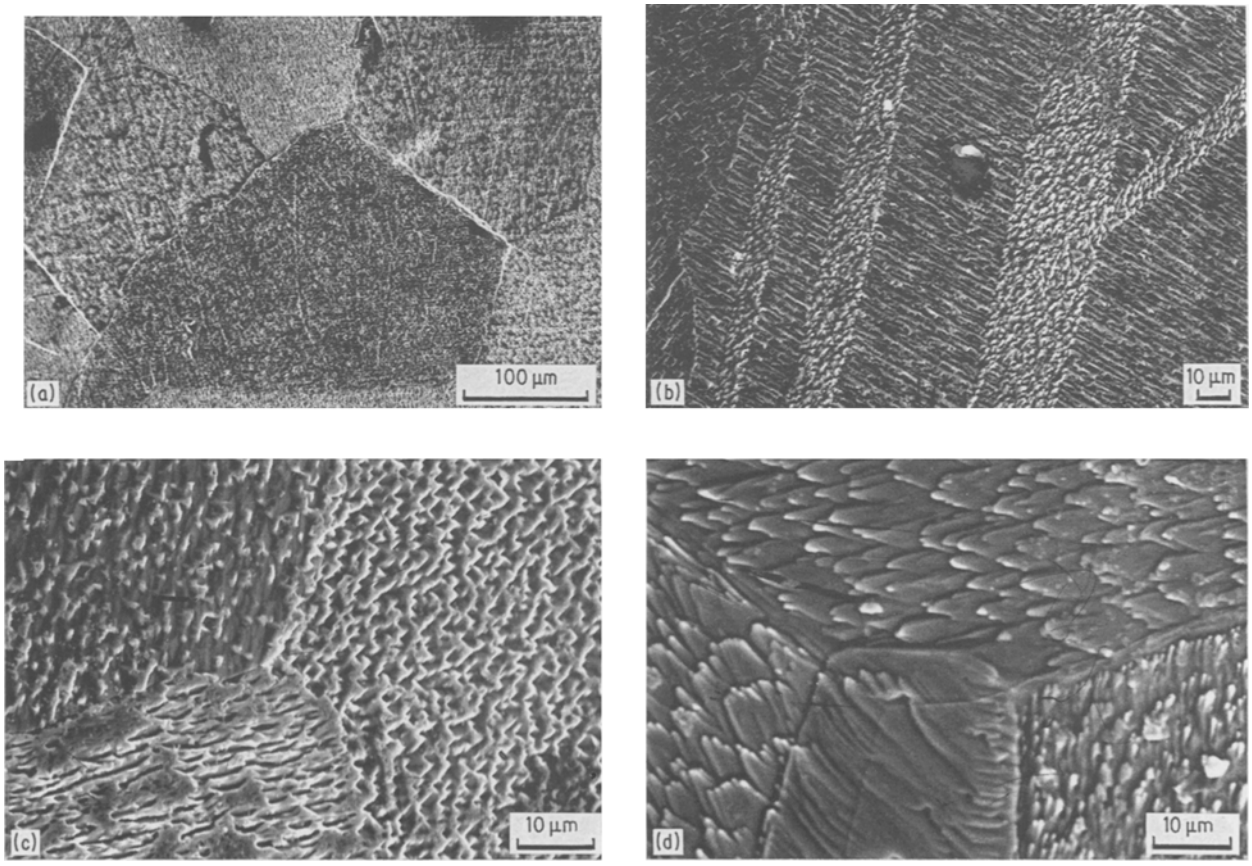

Fig. 6. Tin anode surface following polarization at −0.51 V for 20 min in 0.5 M NaCl.

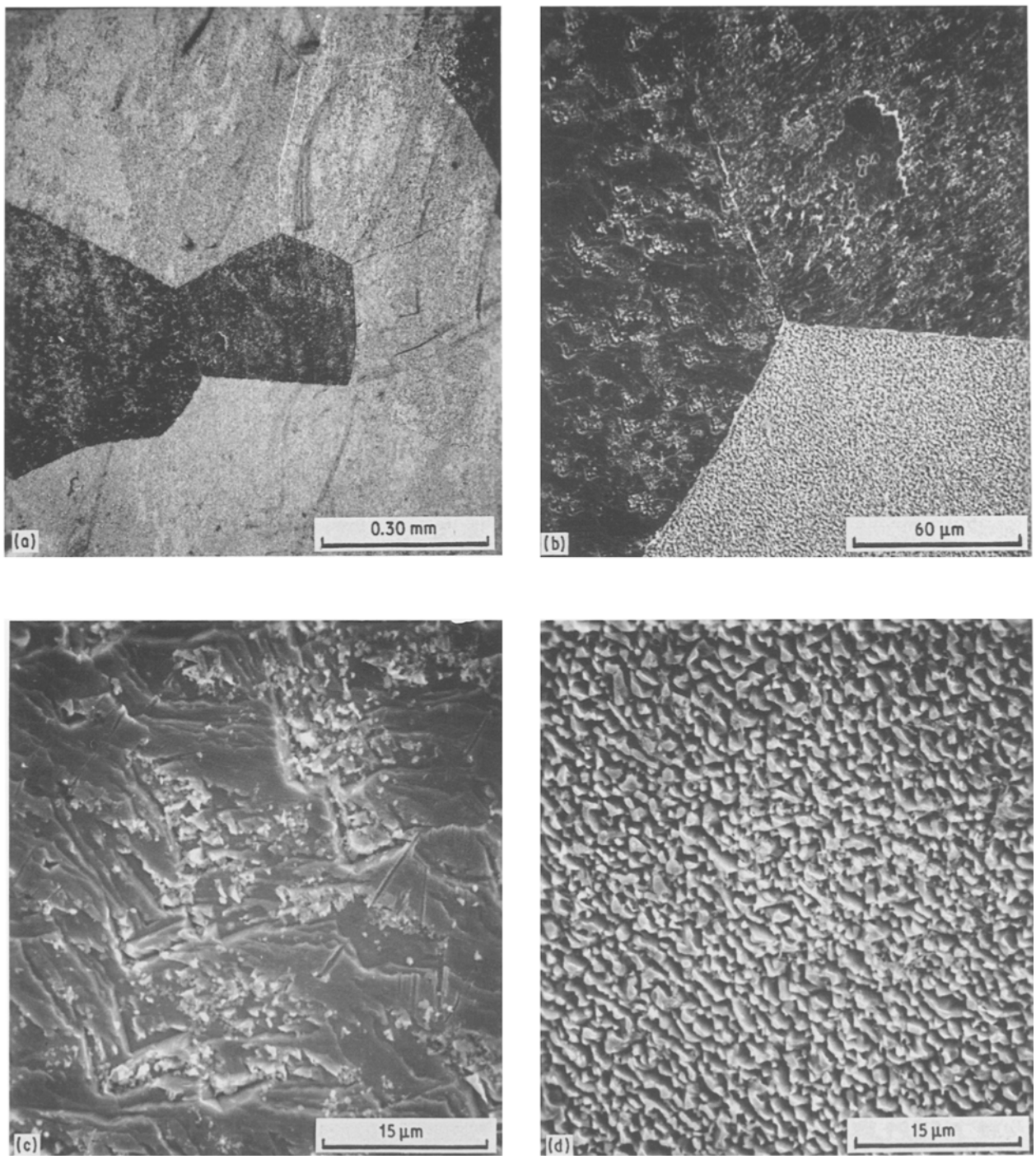

Fig. 7. Tin anode surface following polarization at −0.47 V for 20 min in 0.5 M NaCl.

very slowly with time, its value being $\approx 0.3\,mA\,cm^{-2}$ at $t = 0$ compared to $\approx 0.25\,mA\,cm^{-2}$ at $t \approx 20$ min.

The log i_{ss} values are plotted against E in Fig. 3, i_{ss} being the steady-state current density values under potentiostatic control. The log i_{ss} vs E curves at $\omega = 1000$ rpm are given at five concentrations ranging from 0.1 to 1 M NaCl. A linear relationship log i_{ss} vs E is observed for $E < -0.5$ V, the Tafel slope being $\approx 40\,mV\,decade^{-1}$ regardless of the NaCl concentration, i.e.

$$\left(\frac{\partial E}{\partial \log i_{ss}}\right)_{a_{Cl^-}} = 40\,mV\,decade^{-1} \qquad (8)$$

The order of reaction with respect to Cl^- activity is 0.9 in the Tafel region (Fig. 4), i.e.

$$\left(\frac{\partial \log i_{ss}}{\partial \log a_{Cl^-}}\right)_E = 0.9 \qquad (9)$$

In addition, the variation of ω from 400 to 6000 rpm has practically no influence on the log i_{ss} vs E curves illustrated in Fig. 3, from which it is deduced that the rate-determining step (r.d.s.) of the electrodissolution mechanism of tin in region II is not a mass transfer process in the solution. The Tafel behavior of the log i_{ss} vs E curve for $E \leqslant -0.50$ V supports the idea that the r.d.s. is a charge transfer process.

In the present investigation, the Tafel slope value of $40\,mV\,decade^{-1}$ is significantly different from values

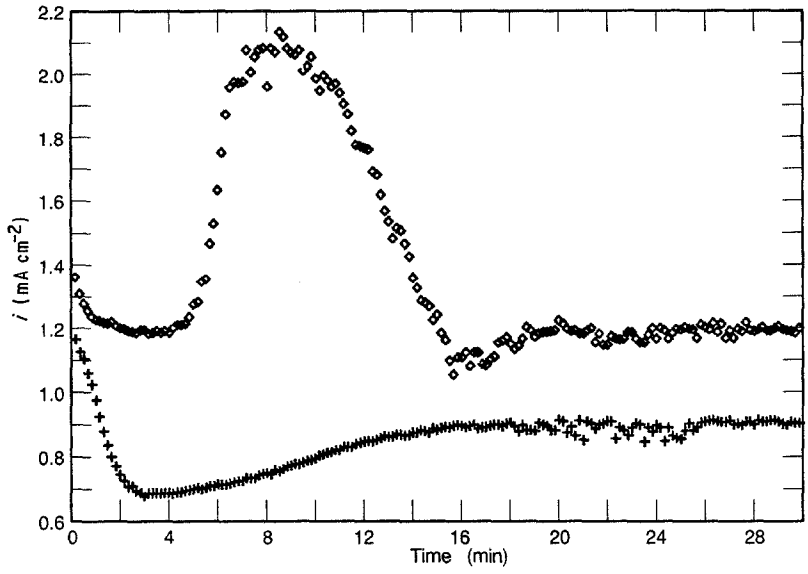

Fig. 8. Current vs time transients in 0.5 M NaCl solution at −0.49 (◇) and −0.47 (+) V. ω = 1000 rpm. The potential step starts from E_{corr}.

cited in the literature [12, 15]. Johnson and Liu [12] reported 30 mV decade^{-1} for the anodic dissolution of tin in acidic chloride solutions at pH $\leqslant$ 2.9 while Stirrup and Hampson [15], under approximately the same experimental conditions (pH $\leqslant$ 2.9), reported 64 mV decade^{-1}. A Tafel slope of 30 mV decade^{-1} is associated with a reaction sequence having a chemical r.d.s. preceded by two charge transfer steps at equilibrium, the generated species being $SnCl_3^-$. The value of 64 mV decade^{-1} is explained by the simultaneous transfer of two electrons as r.d.s., the generated species being $SnCl_3^+$.

The fact that $(\partial \log i_{ss}/\partial \log a_{Cl^-})$ is close to one at pH 4 promotes the idea that $SnCl^+$ species are generated during the electrodissolution of tin. The following mechanism with the surface formation of chemisorbed $SnCl^+$ species is therefore tentatively proposed, at pH 4:

$$Sn + Cl^- = (SnCl)_{ads} + e \quad \text{step 1} \quad (10)$$

$$(SnCl)_{ads} \longrightarrow SnCl^+ + e \quad \text{step 2 (r.d.s.)} \quad (11)$$

This process involves two consecutive steps, each corresponding to the transfer of one electron: step 1 is close to equilibrium with production of $(SnCl)_{ads}$ as an intermediate, whereas step 2 (the r.d.s.) corresponds to the electrochemical oxidation of $(SnCl)_{ads}$ with generation of $SnCl^+$ species.

Under Langmuir isotherm conditions, the degree of coverage of the surface by $(SnCl)_{ads}$, i.e. θ, is ≈ 1, since step 1 is significantly faster than step 2. A Tafel slope of 120 mV decade^{-1} is deduced from this mechanism, i.e. with $\theta \approx 1$ and a transfer coefficient $\alpha = 0.5$ [16]. Under the Temkin isotherm conditions, $0.1 \leqslant \theta \leqslant 0.9$ while θ changes with the applied potential. A Tafel slope of 40 mV decade^{-1} is associated with step 2 ($\alpha = 0.5$) as r.d.s. under Temkin adsorption conditions [16]. The fact that $(\partial E/\partial \log i_{ss})_{a_{Cl^-}}$ = 40 mV decade^{-1} (Fig. 3) and $(\partial \log i_{ss}/\partial \log a_{Cl^-})$ is ≈ 1 (Fig. 4) with the dissolution current of tin being practically independent of ω is in good agreement with characteristics derived from the dissolution mechanism tentatively proposed above, i.e. Equations 10 and 11 under Temkin adsorption conditions [16].

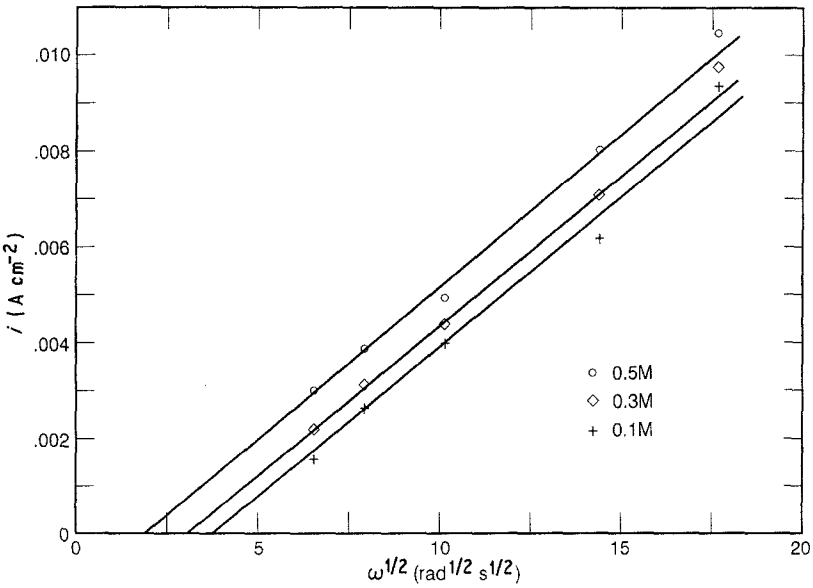

Fig. 9. Current density in the current plateau region vs the square root of the angular velocity of the electrode.

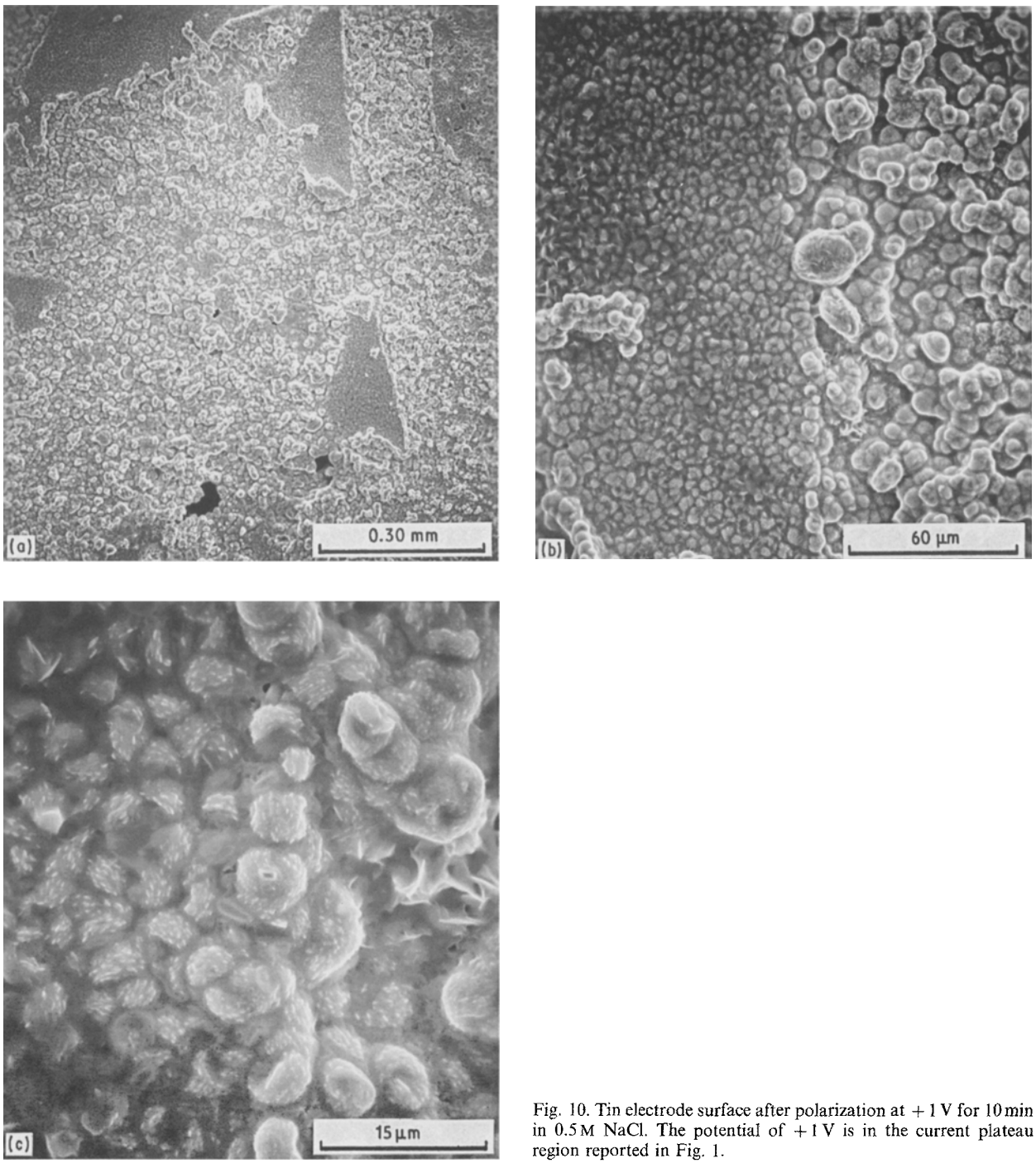

Fig. 10. Tin electrode surface after polarization at + 1 V for 10 min in 0.5 M NaCl. The potential of + 1 V is in the current plateau region reported in Fig. 1.

SEM examination of the tin surface revealed the following characteristics.

(1) The grain diameter varies from $\approx 50\,\mu m$ to $\approx 400\,\mu m$ as seen in Fig. 5, where the surface shown is that prior to immersion.

(2) The metal surface is bare. Its morphology is related to the orientation of the individual grains (Fig. 6) after polarization in the Tafel region. In Fig. 6, the tin was polarized for 20 min in 0.5 M NaCl solution under an applied potential of -510 mV, which is close to the upper limit potential of the Tafel region, i.e. ≈ -500 mV (Fig. 3).

At applied potentials more anodic than ≈ -500 mV, log i_{ss} vs E does not indicate a Tafel relationship (Fig. 3) since the measured i_{ss} values are significantly lower than those extrapolated from the log i_{ss} vs E curve observed in the Tafel region. This behavior is associated with partial surface coverage by a corrosion product as seen in Fig. 7, where tin was polarized at -470 mV for 20 min in 0.5 M NaCl solution. The black spots are practically free of any corrosion product but the white ones are entirely covered by a precipitate. The compound envisaged from the potential–pH diagrams reported in the literature [2] in this range of chloride ion concentrations and potentials at pH 4 is $SnOHCl \cdot H_2O$. X-ray microanalysis of the precipitate reveals 1 atom of Sn for 1 atom of Cl, which is consistent with the formation of $SnOHCl \cdot H_2O$ compound. In addition, the shape of the current vs time transients curve is largely influenced by

an increase of the applied potential as soon as the precipitate becomes accumulated on the electrode surface (Fig. 8). In Fig. 8 the precipitate is formed at $E = -0.47$ V to be practically absent at $E = -0.49$ V.

3.3. *Plateau current region (region IV)*

At concentrations of 0.1–1 M NaCl, the plateau current observed in region IV (Fig. 1) is independent of the sweep rate and rises as the chloride ion concentration increases. The plateau current values are plotted against the square root of ω at 0.1, 0.3 and 0.5 M NaCl concentration in Fig. 9. Linear relationships of i vs $\omega^{1/2}$ are observed:

at 0.5 M NaCl concentration

$$i\,(\mathrm{A\,cm^{-2}}) = -0.00116 + 0.00062\omega^{1/2}\,(\mathrm{rad^{1/2}\,s^{-1/2}}) \quad (12)$$

at 0.3 M NaCl concentration

$$i\,(\mathrm{A\,cm^{-2}}) = -0.0019 + 0.00062\omega^{1/2}\,(\mathrm{rad^{1/2}\,s^{-1/2}}) \quad (13)$$

at 0.1 M NaCl concentration

$$i\,(\mathrm{A\,cm^{-2}}) = -0.00225 + 0.00062\omega^{1/2}\,(\mathrm{rad^{1/2}\,s^{-1/2}}) \quad (14)$$

This behavior indicates that the diffusion of an ionic species into the solution is the r.d.s. of the dissolution process in this region of potential. The negative values of i at $\omega = 0$ are ascribed to the presence of a porous corrosion product on the surface (Fig. 10). The morphology of the corrosion product formed during the dissolution of tin is very different in regions II and IV (Figs 8 and 10). Since the slope $\partial i/\partial\omega^{1/2}$ is independent of the chloride ion concentration, it may be concluded that the diffusing species differ in nature from chloride ions.

4. Conclusions

The corrosion potential of tin is slightly cathodic with respect to the reversible potentials of the Sn/SnO and Sn/SnO_2 couples. The corrosion current remains at $\approx 1.7\,\mu\mathrm{A\,cm^{-2}}$ regardless of the NaCl concentration.

The anodic dissolution of tin displays Tafel behavior as long as the electrode surface is bare. A dissolution mechanism is tentatively proposed from which the main characteristics for tin can be derived, i.e.

$$\left(\frac{\partial E}{\partial \log i}\right)_{a_{Cl^-}} = 40\,\mathrm{mV\,decade^{-1}},$$

$$\left(\frac{\partial \log i}{\partial a_{Cl^-}}\right)_E \approx 1 \quad \text{and} \quad \left(\frac{\partial i}{\partial \omega}\right)_{E,a_{Cl^-}} \approx 0.$$

Partial coverage of the surface by a corrosion product is observed for E values anodic to ≈ -0.5 V vs SCE and the anodic dissolution no longer displays Tafel behavior.

From +0.4 to 1 V, a plateau current is observed on the log i vs E curves and the anode is completely covered by a corrosion product. The use of a rotating disc electrode in this region of potential suggests that the rate-determining step of the tin dissolution process is the diffusion of an ionic species into the solution.

Acknowledgements

The authors would like to acknolwedge the financial support of the Institut de recherche d'Hydro-Québec (IREQ) and their gratitude to Dr A. K. Vijh (IREQ) for useful discussions.

References

[1] M. Pourbaix, 'Atlas of Electrochemical Equilibria', Pergamon, Oxford (1966) p. 475.
[2] C. I. House and G. H. Kelsall, *Electrochim. Acta* **29** (1984) 1459.
[3] A. Ya. Chatalov, *Dokl. Akad. Nauk. SSSR* **86** (1952) 775.
[4] Z. Galus, in 'Encyclopedia of Electrochemistry of the Elements' (edited by A. Y. Bard), Dekker, New York (1973).
[5] S. C. Britton, 'Tin Versus Corrosion', International Tin Research Institute Publication No. 510, London (1975).
[6] W. E. Boggs, R. H. Kachik and G. E. Pellissier, *J. Electrochem. Soc.* **108** (1961) 6.
[7] W. E. Boggs, P. S. Trozzo and G. H. Pellissier, *ibid.* **108** (1961) 13.
[8] W. E. Boggs, *ibid.* **108** (1961) 124.
[9] R. Steinherz, *Z. Electrochem.* **30** (1924) 279.
[10] V. A. Khitzov and V. I. Shatalova, *Zh. Prikl. Khim.* **34** (1961) 2001.
[11] T. P. Hoar, *Trans. Faraday Soc.* **124** (1937) 1152.
[12] J. W. Johnson and E. C. Liu, *J. Less Common Metals* **34** (1974) 113.
[13] M. L. Rumpel, A. W. Davidson and J. Kleinberg, *Inorg. Chem.* **3** (1964) 935.
[14] M. E. Straumanis and M. Duta, *ibid.* **5** (1966) 992.
[15] B. N. Stirrup and N. A. Hampson, *J. Appl. Electrochem.* **6** (1976) 353.
[16] B. E. Conway, 'Theory and Principles of Electrode Processes', The Ronald Press Co., New York (1965) Chap. 8.